Exploration of CH···π interactions involving the π-system of pseudohalide coligands in metal complexes of a Schiff-base ligand

Exploration of CH···π interactions involving the π-system of the pseudohalide coligands in metal complexes of a Schiff-base and studies of their photophysical properties

Prateeti Chakraborty,[a,*] Suranjana Purkait,[a] Sandip Mondal[a], Antonio Bauzá,[b] Antonio Frontera,[b,*] Chiara Massera,[c] and Debasis Das,[a,*]

[a]*Department of Chemistry, University of Calcutta, 92 A. P. C. Road, Kolkata-700 009, India, E-mail: dasdebasis2001@yahoo.com*

[b]*Departament de Química, Universitat de les Illes Balears, Crta. De Valldemossa km 7.5, 07122 Palma (Baleares), Spain, E-mail: toni.frontera@uib.es*

[c]*Dipartimento di Chimica, University of Parma, Parco Area delle Scienze 17/A, 43124 Parma, Italy*

A series of four mononuclear Schiff-base complexes, namely $[Zn(L)(NCS)_2]$ (**1**); $[Zn(L)(N_3)_2]$ (**2**); $[Cu(L)(NCS)_2]$ (**3**) and [Ni (L)(2bpy)(NCS)](ClO_4)] (**4**), [where L = N,N-Dimethyl-N′-(phenyl-pyridin-2-yl-methylene)-ethane-1,2-diamine and 2bpy = 2-benzoylpyridine] were synthesized with the aim to investigate the role of different non-covalent weak interactions responsible for the crystal packing of the complexes. All of them were structurally characterised by X-ray diffraction analysis. In addition to conventional $CH_3\cdots\pi$ and $\pi\cdots\pi$ interactions, the importance of unconventional C–H$\cdots\pi$ interactions in the crystal packing of compounds **1**–**4** was investigated by means of Hirshfeld surface analysis and DFT calculations. In these unconventional C–H$\cdots\pi$ interactions the π-system (electron donor) is provided by the pseudohalide coligands. The interactions formed by the π-system depend on the nature of the pseudohalide (N_3, NCO, NCS or NCSe) as demonstrated by Molecular Electrostatic Potential calculations. Additionally, we have explored the photophysical properties of the complexes. Finally, we have combined a search in the Cambridge Structural Database and DFT energy calculations to analyse the rare ambidentate behaviour of SCN within the same complex.

Introduction

With the advancement of supramolecular chemistry in the last few decades much attention has been given to the study of different non covalent interactions,[1-6] one of the main foundation pillars of supramolecules. It is now well recognized that non covalent interactions are often ubiquitous[7-11] and, although of very small ~~in~~ magnitude, very much significant to influence the structural topology and consequently several physical and chemical characteristics of the systems. Extensive investigations on non covalent interactions like hydrogen bonding, halogen bonding, van der Waals forces, polar attractions, hydrophilic-hydrophobic interactions etc., in protein and even small organic moieties are underway,[12-13] but similar investigations on coordination complexes are very scattered.[14-15] However, it is very much crucial to elucidate the finer details of the several non covalent interactions present in coordination complexes of metal ions to shed light on the origin of observed topology, coordination behaviour of the ligands and physical and chemical properties of the species.[16,17] In order to achieve truly fruitful evidence, a proper fusion of experimental and theoretical studies is utmost essential.[18] In our initial attempt, we have selected two pseudohalides, SCN and N_3 as coligands, one Schiff-base ligand, N,N-Dimethyl-N′-(phenyl-pyridin-2-yl-methylene)-ethane-1,2-diamine (L) and three bio-relevant metal ions, Zn(II), Cu(II) and Ni(II) as metal centres. The selection of the coligands lies on their versatile modes of coordination[19-32] which may lead to interesting structural features as well as to some uncommon non-covalent interactions. The Schiff-base has been chosen to strengthen the possibility of observing several interesting non-covalent interactions like cation-π, anion-π, CH-π etc.[33-37] The choice of the aforesaid metal ions is mainly to exploit their Lewis acidity to influence the non-covalent interactions and the physiochemical properties of the complexes. The reaction of the chosen Schiff-base with metal perchlorates followed by addition of NaX (X= SCN and N_3) yielded four complexes, namely **[Zn(L)(NCS)$_2$] (1)**; **[Zn(L)(N$_3$)$_2$] (2)**; **[Cu(L)(NCS)$_2$] (3)** and **[Ni(L)(2bpy)(NCS)](ClO$_4$)] (4)**. Our all efforts to prepare the N_3 analogues of **3** and **4** were unsuccessful. Single crystal X-ray diffraction followed by Hirshfeld surface analysis revealed the existence of unprecedented CH-π interactions along with other weak forces. More importantly, in complex **3** two thiocynato moieties remain coordinated via two different sites, *viz* via S- and via N-sites, a rare finding in Schiff-base complexes of Cu(II). Thorough DFT analyses have

been performed to rationalize the observed unprecedented non-covalent interactions and the finding of the rare ambidentate behaviour of SCN. Since the ligand L contains a pyridine moiety as well as extended conjugation, we have extensively investigated the photoluminescence behaviour of the ligand and the complexes.

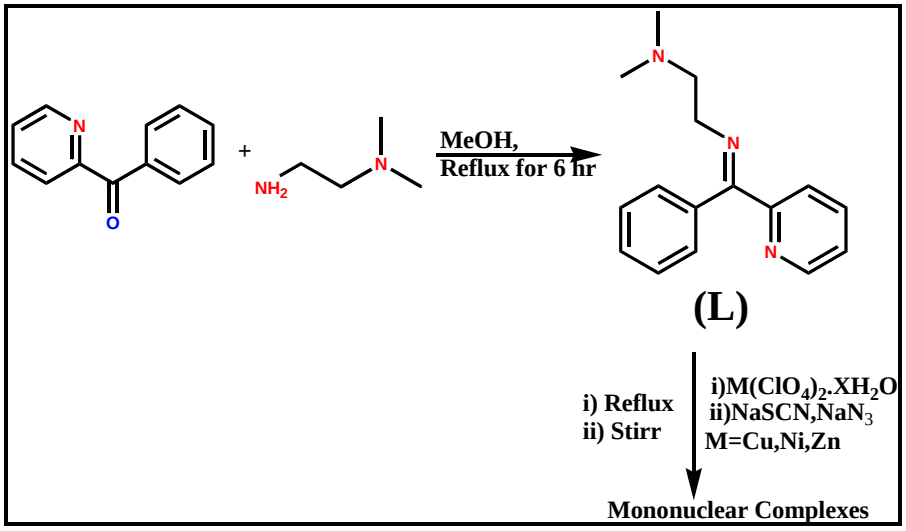

Scheme 1: Synthetic route of the complexes.

Results and discussion

Synthesis and characterization

All the four complexes were prepared by following a template synthetic technique. FT-IR spectral studies reveal that all the complexes exhibit bands due to C=N stretching in the range 1630-1648 cm^{-1} and skeletal vibration in the range 1545-1555 cm^{-1}. The observed sharp band at nearly 2100 cm^{-1} in complexes **1**, **3** and **4** clearly indicates the presence of thiocyanate in one binding mode. Complex **2** exhibits a sharp band near 2200 cm^{-1} due to presence of azide anions in the complex.

Crystal structure description of the complexes

Complex [Zn(L)(NCS)$_2$] (1). The molecular structure of the mononuclear complex **1** is shown in Fig.1. The metal center is pentacoordinated to five nitrogen atoms belonging to the tridentate ligand L and to two thiocyanate groups. The geometry can be best described as distorted square pyramidal (with the nitrogen atom N4 in apical position), as evidenced by the tau-factor[38] of 0.30 (τ = 1 for a perfectly trigonal bipyramidal geometry, τ = 0 for a perfectly tetragonal geometry). Relevant distances and angles are summarized in Table 1, showing normal ranges of the Zn-N bond

lengths for this class of compounds. The distortion of the geometry is evidenced by the values of the equatorial angles spanning from 75.0(3) to 96.2(4)°.

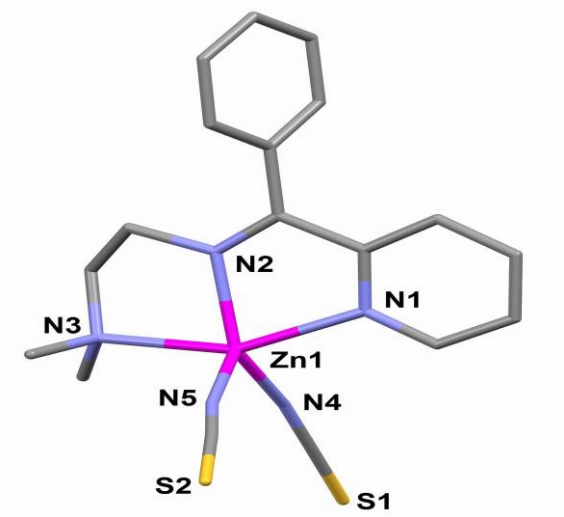

Fig. 1 Molecular structure of **1** with partial atom numbering scheme. Hydrogen atoms have been omitted for clarity.

The complexes form dimers along the *c* axis of the unit cell, through π···π stacking interactions between the coordinated pyridine rings (centroid…centroid distances of 3.885(3) Å, see Fig. S8). The phenyl moiety of the ligand and the methylenic hydrogens of the ethane backbone are also involved in CH–π interactions [C···centroid = 3.899(4) Å; C-H···centroid 147.21°].

Table 1. Selected geometric parameters (Å, °) for compound **1.**

Zn1–N1	2.205(7)	N1–Zn1–N3	151.6(3)
Zn1–N2	2.078(8)	N2–Zn1–N4	133.9(4)
Zn1–N3	2.289(8)	N1-Zn1-N4	94.8(4)
Zn1–N4	1.977(9)	N2-Zn1-N3	78.5(3)
Zn1–N5	1.986(9)	N3-Zn1-N4	96.2(4)
		N1-Zn1-N2	75.0(3)

Complex [Zn(L)(N_3)$_2$] (2). The molecular structure of complex **2** is very similar to that of **1**, the only difference being the presence of two azido groups replacing the thiocyanate anions (see Fig. 2). Complex **2** crystallizes in the triclinic space group *P-1* as two independent complexes (tagged with the letters A and B), displaying ~~the~~ similar geometrical values (see Table 2 for selected distances and angles). The metal

centers are penta-coordinated to five nitrogen atoms in a distorted square pyramidal environment (with a tau-factor of roughly 0.40), in which the atoms N4A and N4B occupy the apical positions. Also in this case the equatorial angles deviate significantly from the theoretical values (see Table 2). Both the two independent complexes A and B form hydrogen bonds with the lattice water molecules *via* the terminal nitrogen atoms of the azido groups [O1W···N6A 2.860(5)Å; O1W···N6B[a] 2.968(5) Å; a = x-1,+y,+z] ((see Figure S9 in the Supporting Information).).

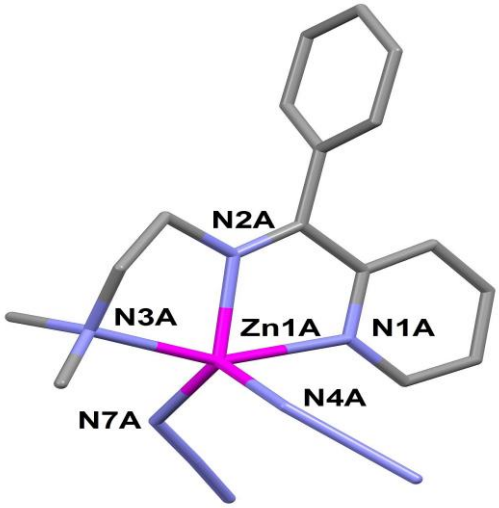

Fig. 2 Molecular structure of one of the two independent complexes in **2** with partial atom numbering scheme. Hydrogen atoms and water lattice molecules have been omitted for clarity.

Table 2. Selected geometric parameters (Å, °) for compound **2.**

Zn1A–N1A	2.277(2)	Zn1B–N1B	2.277(2)
Zn1A–N2A	2.074(2)	Zn1B–N2B	2.084(2)
Zn1A–N3A	2.196(2)	Zn1B–N3B	2.184(2)
Zn1A–N4A	1.980(2)	Zn1B–N4B	1.987(3)
Zn1A–N5A	1.977(2)	Zn1B–N5B	1.973(2)
N1A–Zn1A–N3A	153.06(7)	N1B–Zn1B–N3B	152.98(7)
N2A–Zn1A–N7A	129.08(8)	N2B–Zn1B–N7B	129.63(7)
N2A–Zn1A–N3A	79.55(7)	N2B–Zn1B–N3B	79.75(7)
N1A–Zn1A–N2A	74.13(7)	N1B–Zn1B–N2B	73.93(8)
N1A–Zn1A–N7A	94.98(8)	N1B–Zn1B–N7B	94.90(9)

N7A–Zn1A–N3A	97.19(8)	N7B–Zn1B–N3B	97.20(9)

In the lattice, the complexes form C-H···π interactions involving the hydrogen atoms belonging to the pyridine moiety and the phenyl ring of the ligand [C-H···centroid 3.741(5) Å; angle 146.09(3)°]. Moreover, complexes of the same type form dimers (either A···A or B···B) trough C-H···π interactions between the coordinated pyridine ring and the hydrogen atoms of the amine methyl groups (Fig. S10, bottom). [C-H···centroid 3.371(6); angle 110.03(3)°].

Complex [Cu(L)(NCS)$_2$] (3). Compound **3** is the previously reported mononuclear complex [Cu(L)(NCS)$_2$] [39] which contains the same number and type of ligands of **1**, but with one of the two thiocyanate groups coordinating through the sulphur atom. In the lattice, the crystal structure is stabilized by C-H···N interactions between the N atom of the S-coordinated thiocyanate ion and the C-H of the phenyl ring [C···N 3.510(2) Å, C-H···N 142.67(6)°], and by S···π interactions (3.753(4) Å (see Fig. 3).

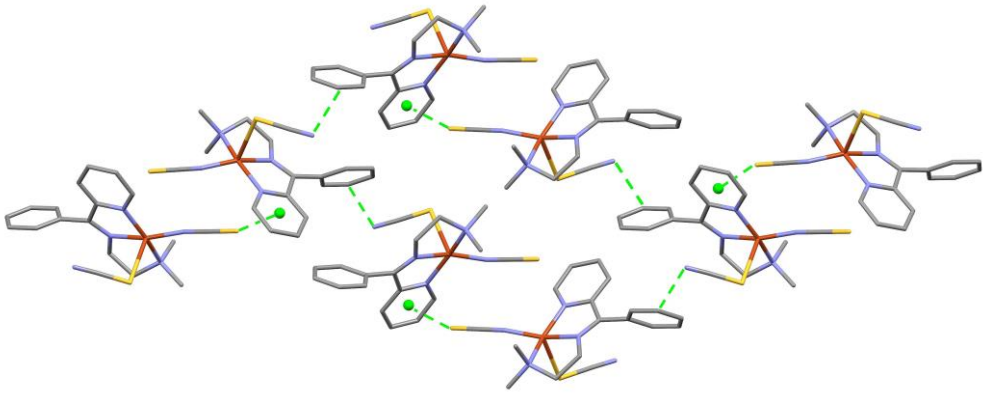

Fig. 3 View along the *a* axis of the packing of compound **3**. C-H···N and S···π interactions are represented as green dotted lines. Centroids are green spheres. Hydrogen atoms have been omitted for clarity.

Complex [Ni(L)(2bpy)(NCS)](ClO$_4$)] (4). The molecular structure of **4** ~~[Ni(L)(2bpy)(NCS)](ClO$_4$)]~~ is shown in Fig. 4. Surprisingly, the coordination environment around the metal comprises the Schiff base ligand L, one thiocyanate ion, and the 2-benzoylpyridine used for preparing the Schiff base.

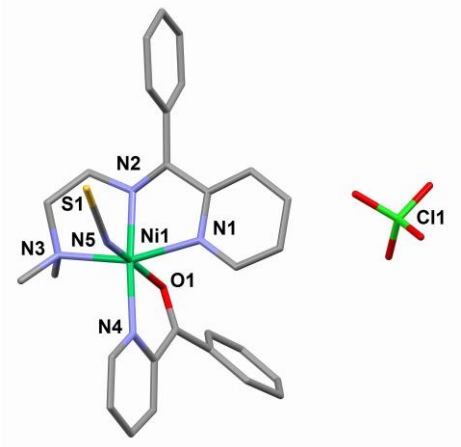

Fig. 4 Molecular structure of **4** with partial atom numbering scheme. Hydrogen atoms have been omitted for clarity.

The remaining positive charge is balanced by the presence of one perchlorate ion located in the lattice. Ni1 is in an octahedral environment formed by the ligand donor atoms N1 and N3 in the equatorial plane, which is completed by the nitrogen atom N5 from the thiocyanate ion and the oxygen atom O1 from benzoylpyridine.

The axial positions are occupied by N2 from the Schiff-base ligand and by N4 belonging to the pyridine moiety, with a N2-Ni-N4 angle of 171.28(9)°. The equatorial angles vary from 85.31(8) to 96.58(9)º revealing a slight distortion of the octahedron. The complexes interact in the lattice forming dimers through π···π interactions between the coordinated pyridine rings belonging to the Schiff base (the centroid···centroid distance is of 3.846(8) Å). These dimers form in turn S···π interactions involving the sulphur atom of the thiocyanate group and the pyridine ring of the 2-benzoylpyridine [S···centroid, 4.105 Å] (see Fig. S11)

Table 3. Selected geometric parameters (Å, °) for compound **4.**

Ni1–N1	2.109(3)	N1-Ni1-N3	159.91(8)
Ni1–N2	2.013(2)	N2-Ni1-N4	171.28(8)
Ni1–N3	2.147(3)	O1-Ni1-N5	169.55(8)
Ni1–N4	2.072(2)	N1-Ni1-N2	78.00(8)
Ni1–O1	2.131(1)	O1-Ni1-N4	76.99(7)
Ni1-N5	2.034(2)	N2-Ni1-N3	81.90(9)

Analysis of crystal packing by the Hirshfeld surface method

Fig. S12-S15 shows the Hirshfeld surfaces for **1-4**, mapped with the d_{norm} property (red and blue areas represent contacts shorter and longer than the van der Waals separations, respectively), along with the neighbouring molecules involved in the closest contacts. However, a better way for summarizing the interactions taking place in the crystal structures of the four compounds is the use of two-dimensional fingerprint plots (Fig. 5) which can be also broken down to highlight the contribution of the different atoms involved.

The fingerprint plot of **1** shows the presence of a diffuse blue region in the top right corner (region of long distances to the nearest atoms), which indicates a lower packing efficiency of **1** with respect to the other complexes. The other main features of the plot are i) the small wings (red circles A and B in Fig. 5) generated by different sets of CH···π interactions (A: the phenyl moiety of the ligand and the methylenic hydrogens of the ethane backbone; B: the phenyl moiety of the ligand and the H atoms of the coordinated pyridine); ii) a region of pale blue/green colour on the diagonal at around $d_e \cong d_i \cong$ 1.8 Å, due to the presence of π···π stacking (black arrow in Fig. 5)

In complex **2**, two different fingerprint plots are present, one for each independent molecule of the asymmetric unit. In the plot of **2A**, the pointed nose and the two little spikes inside it are due to a series of H···H interactions, which contribute to 35.1% of the total Hirshfeld surface (see Fig.6) and which are a common feauture in these type of plots even if in this case they do not contribute to the stabilization of the crystal structure. The other significant features are represented by the two lateral wings (highlighted by green circles) generated by short CH···N interactions of *ca*. 2.5 Å involving the azide ligand. π ···π stacking is, in this case, irrelevant. The plot of **2B** is quite similar to that of **2A**. Also in this case the main features are the central round nose generated by H···H interactions and the lateral wings due to the CH···N interactions. A small extra spike (red arrow) is relative to O···H interactions between the lattice water molecules and the methylenic hydrogen atoms of the ethane backbone (4.5 % of the total Hirshfeld surface).

The fingerprint plot of **3** presents a central nose in the region $d_e \cong d_i \cong$ 1.0 Å, again generated by the H···H interactions involving the hydrogen atoms of the coordinated

pyridines and of the phenyl rings. As observed previously for compound **2**, also in this case two lateral spikes are present (green circles), due to the CH···N interactions of *ca*. 2.6 Å between the aromatic H9 belonging to the phenyl moiety and the terminal azide nitrogen N5. The other important features are the two wings (red arrows) generated by the S···H interactions around 2.9 Å involving the terminal sulphur atom of the thiocyanate ligand and the H atoms of the coordinated pyridine ring.

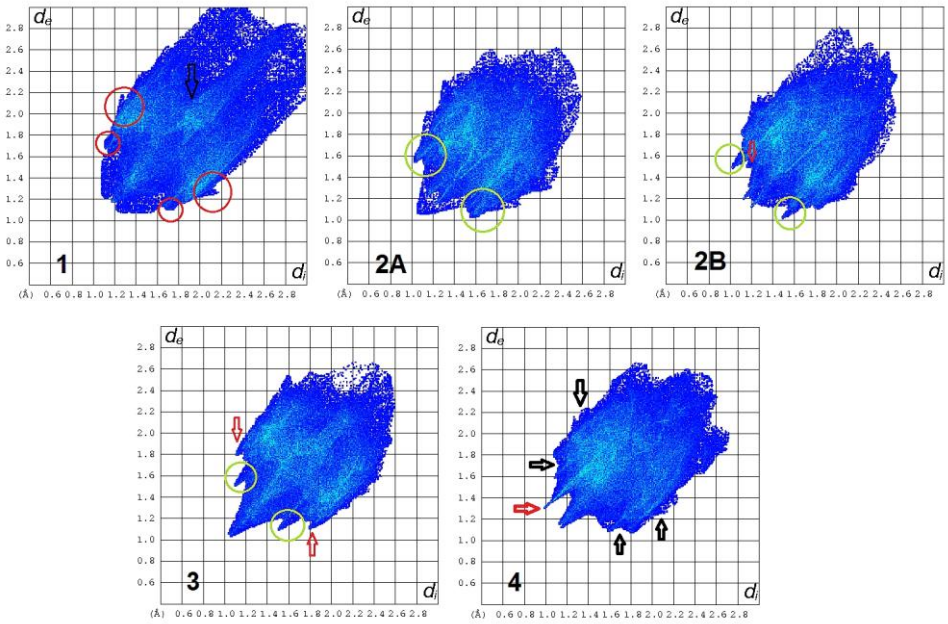

Fig. 5 Comparison of the fingerprint plots of compounds **1-4**.

The fingerprint plot of **4** shows some differences compared to the other ones previously reported, and this is mainly due to the presence of perchlorate ions which contribute to the stabilization of the crystal structure. In particular, the Cl-O···H hydrogen bonds are represented by a sharp spike (red arrow) which is an "asymmetrical" feature of the plot, since the perchlorate ion is always outside the Hirshfeld surface of the complex. The usual H···H sharp nose is present, comprising interactions which contribute 44.9% to the total surface, while the pale blue area with $d_e \cong d_i \cong 1.9$ Å is diagnostic of π···π stacking between the coordinated pyridine rings. Finally, the region of the CH···π interactions is represented by the slight lateral protrusions indicated with black arrows; the π systems involved are both the aromatic rings of the Schiff base and the triple bonds of the thiocyanate ligands.

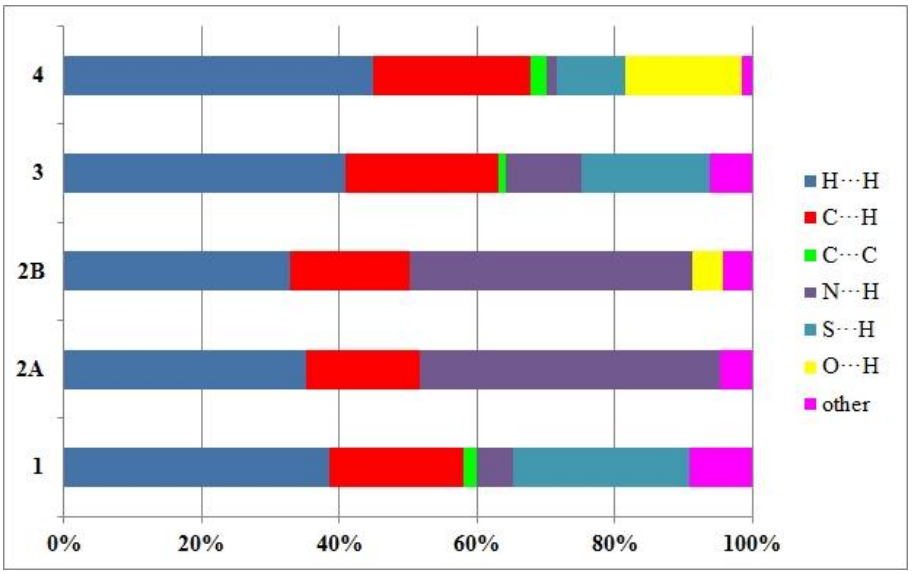

Fig. 6 Contribution (%) of the different intermolecular contacts to the Hirshfeld surface area for **1**-**4**. The detailed numerical values are given in Table S1 of the ESI.

Fluorescence Study

The fluorescence spectra of the ligand as well as of all the four complexes were examined in methanol medium at room temperature.

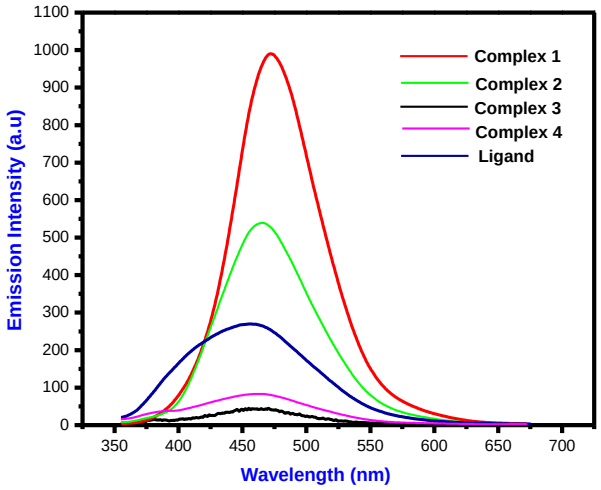

Fig. 7 Fluorescence behavior of the complexes along with the ligand.

Photoexcitations have been performed at λ_{max} of 341 nm. The ligand is very weakly fluorescent in nature due to the π-π^* transition. From the spectrum as well as from

quantum yield calculations (See Table S2) it can be seen that the fluorescence intensity of the ligand is enhanced in complex **1** and complex **2** but quenched in the other two complexes **3** and **4**. The enhancement of the fluorescence behaviour on complexation with zinc is due to the rigidity of the system attained upon complexation.[40] Complex **1** is more fluorescent than complex **2** due to the greater π-π interaction in the complex.

Theoretical Study

We have performed a theoretical study of the non-covalent interactions observed in the solid state of complexes **1-4** and some other interesting geometrical characteristics of the complexes that have been compared to data retrieved from the CSD.

Compounds 1 and 2. Both compounds form interesting self-assembled dimers in the solid state stabilized by a combination of two interactions involving the aromatic rings and the pseudohalides ligands. That is, in the dimeric complex **1** the coordinated pyridine rings form a π–π stacking interaction and, simultaneously an aromatic hydrogen atom of the pyridine interacts with the π-system of the pseudohalide pointing to the central carbon atom. Similarly, in the self-assembled dimer of complex **2** a double $CH_3\cdots\pi$ interaction is observed and, concurrently, one hydrogen atom of the methylene group also points to one atom of the azide. The interaction energies of both dimers are shown in Fig. 8.We have used some additional theoretical models to investigate the strength of each interaction separately and also the influence of the coordination of the pyridine to the Zn(II) metal center on the strength of the π–π and $CH_3\cdots\pi$ interactions in compounds **1** and **2**, respectively. These results are included in the ESI (see Fig. S16)

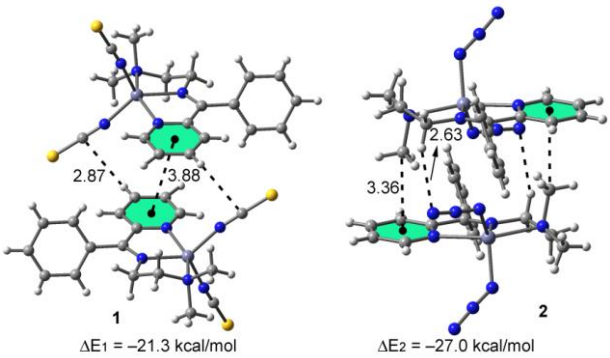

Fig. 8 Self-assembled dimers observed in the solid state of compounds **1** and **2**.

Compound 3. For this compound the theoretical study is devoted to rationalize the different coordination mode of the thiocyanate ligands around the Cu^{II} metal center. One ligand is bonded through the sulfur atom whilst the other one through the nitrogen atom (see Fig. 3). Despite the fact that the linkage isomerism of thiocyanate is well known,[41-43] we have performed a search in the Cambridge Structural Database (CSD) in order to achieve a better understanding of the different binding modes of the thiocyanate anion (monodentate, not bridging ligand) and to know if the Cu–coordination using the sulfur atoms is uncommon. It is well-known that the CSD is a convenient and reliable tool for analyzing geometrical parameters.[44] Interestingly, we have found only 33 X-ray structures (44 fragments) where SCN is coordinated to Cu through the S atom (Cu•••SCN). In these structures a coexistence of the two binding modes is observed, as is the case of compound **3**. It should be mentioned that we have eliminated those hits from the searches where the SCN is acting as bridging ligand in any of the two modes represented in Fig. 12 (inset figs). In sharp contrast, we have found 555 X-ray structures (802 fragments) where the SCN is coordinated to Cu through the N atom (Cu•••NCS). For this search we have also eliminated those hits where the SCN ligand is simultaneously coordinated to more than one metal center. The histogram plots represented in Fig. 12 clearly show a preference of the coordination via the nitrogen atom, due to the significantly larger number of hits observed for this coordination mode. Another interesting aspect is the dissimilar coordination angle observed for each type of complex. In the Cu–SCN histogram plot, it can be observed a preference for a Cu-S-C angle between 90 and 110 degrees and in the Cu–NCS plot a wider range of values is observed centered around a Cu-N-C angle of 165 degrees.

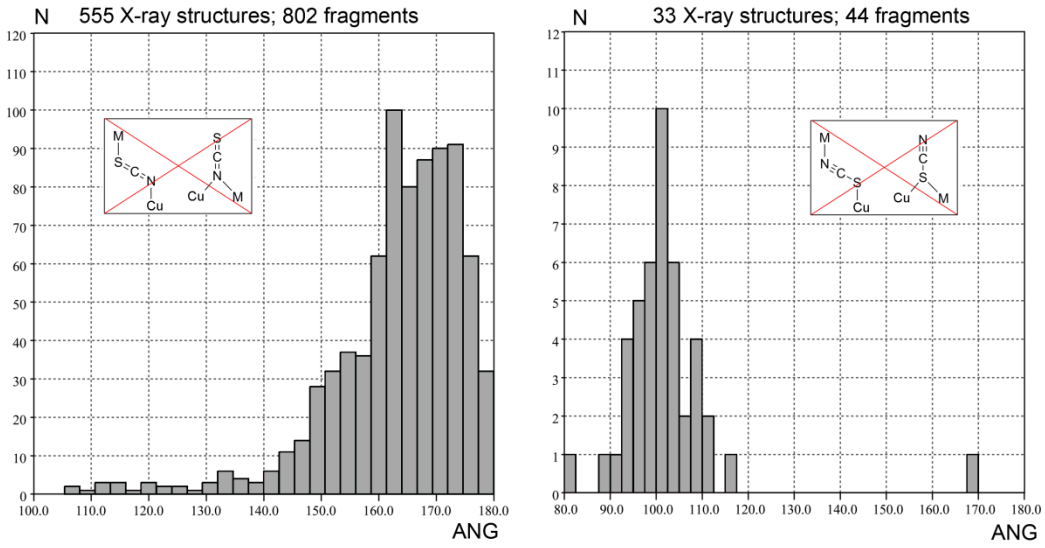

Fig. 12 Histogram plots of Cu-NC (left) and Cu-SC (right) angles in Cu–NCS and Cu–SCN complexes.

We have further analyzed and rationalized the results obtained from the CSD searches using theoretical calculations that we have included in the ESI. DFT calculations show that the coordination through the N atom is 12.7 kcal/mol more favorable than the coordination through the S atom. Consequently, we have further examined the X-ray structure of complex **3** in order to explain the presence of one thiocyanate ligand S-coordinated to the Cu(II) ion that is energetically unfavorable compared to the other coordination mode (see ESI). In the solid state this S-coordinated ligand only establishes a C-H···π interaction similar to what was previously described for the Zn complexes **1** and **2**. In contrast the N-coordinated ligand does not participate in non-covalent interactions. The MEP surface of the $Cu(SCN)_2$ theoretical model shows a negative potential in the direction of the C-H···π interaction. Interestingly the interaction energy obtained using the crystal fragment shown in Fig. 13 (left) is ΔE_3 = –11.8 kcal/mol, which is large and negative in agreement with the short C–H···N distance (2.73 Å). Moreover, this energy is very similar to the energetic difference obtained for the $Cu(NCS)_2$ and Cu(NCS)(SCN) isomers (12.7 kcal/mol, see Figure S15). Therefore the unfavorable S-coordination of the ligand observed in compound **3** is compensated by the C-H···π interaction established by this ligand in the solid state.

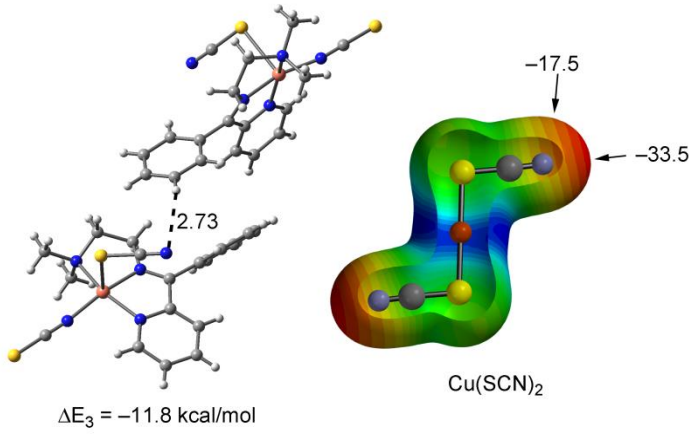

Fig. 13 Left: Fragment of the X-ray structure of compound **3** with indication of the C–H···π interaction. Right: MEP surface of $Cu(SCN)_2$ and the potential energy values at two points of the surface in kcal/mol.

Compound 4. This compound forms an interesting supramolecular self-assembled dimer in the solid state stabilized by a combination of π–π stacking and C–H···π interactions. The π–π stacking interaction is formed by an anti-parallel arrangement of the coordinated pyridine moieties. The double and C-H···π interaction is formed between the meta-hydrogen atom of the pyridine ring and the phenyl ring (see Fig.14). We have also used two theoretical models to investigate the strength of each interaction separately and also the influence of the coordination of the pyridine to the Ni(II) metal center on the strength of the π–π interaction. The interaction energies of the theoretical models are shown in Fig. 14. In particular, we have computed the interaction energies of the dimer retrieved from the X-ray structure (ΔE_4 = –24.9 kcal/mol) and of the two hypothetical dimers based on it. In one of them the phenyl ring has been replaced by a hydrogen atom to calculate the contribution of the CH···π interactions (Fig. 14, middle). As a result, this interaction energy (denoted as ΔE_4') is –11.5 kcal/mol and the difference with ΔE_4 (i.e., –13.4 kcal/mol) gives the contribution of both CH···π interactions. In the other hypothetical dimer of **4** both Ni(II) and the counterions have been removed in order to know the influence of the metal center on the π–π stacking interaction. The resulting interaction energy is ΔE_4'' = –7.8 kcal/mol that is slightly less favorable than ΔE_4'. Thus the influence of the metal coordination upon the π–π stacking interaction is modest and favorable.

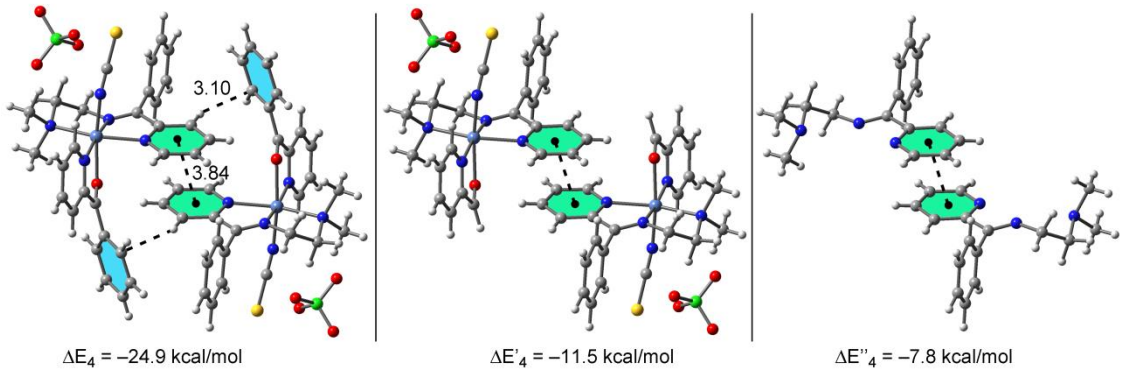

Fig. 14 Left: the self-assembled dimer observed in the solid state of compound **4** Middle and right: Theoretical models of compound **4** and their interaction energies

Experimental

Physical Methods and Materials

Elemental analyses (carbon, hydrogen and nitrogen) were performed using a Perkin–Elmer 240C elemental analyzer. Infrared spectra were recorded on KBr disks (400–4000 cm^{-1}) with a Perkin–Elmer RXI FTIR spectrophotometer. Electronic spectra (200-800 nm) were measured at room temperature on a Shimadzu UV-3101PC by using dry methanol as medium. High purity Copper, Nickel, Zinc perchlorate and sodium thiocyanate were purchased from Fluka; 2-benzoylpyridine from Lancaster,UK; N,N-dimethylethylenediamine from Alfa-Aesar. All other chemicals were of AR grade and used as received. Thermal analyses (TG–DTA) were carried out on a TGA/SDTA851^{e} METTLER-TOLEDO thermal analyzer in flowing dinitrogen (flow rate: 40 cm^3 min^{-1}) at a rate of 10°C per min. Fluorescence spectra of the ligand and of the complexes were recorded in DMF solution with a Perkin-Elmer model LS 55 Luminescence spectrometer.

Synthesis of the complexes

All the complexes were synthesized adopting a template synthetic technique where metal perchlorate salts $M(ClO_4)_2$,(M= Ni, Cu and Zn) were allowed to react with the Schiff-base ligand formed *in situ* via the condensation of 2-benzoylpyridine (0.183 gm,1 mmol) and N,N-dimethylethylenediamine (0.088 gm, 1 mmol).

Syntheses of complex $[Zn(L)(NCS)_2]$ (1).

To a methanolic solution (20 mL) of N,N-dimethylethylenediamine (0.088 gm, 1 mmol) a methanolic solution of 2-benzoylpyridine (0.183 gm,1 mmol) was added and refluxed for 6 hr. After that a methanolic solution of zinc perchlorate hexahydrate

(0.372 g, 1 mmol) was added ~~to it~~ and the resulting solution was allowed to stir for 3 hr. Subsequently, an aqueous solution of sodium thiocyanate (0.162 g, 2 mmol) was added dropwise with constant stirring and the stirring was continued for an additional period of 2 hr. The mixture was then filtered and the filtrate ~~was~~ kept in a $CaCl_2$ desiccator. Light yellow single crystals suitable for X-ray analysis were obtained from the filtrate after few days. (Yield: 87 %). Anal. Calcd.: $C_{18}H_{19}ZnN_5S_2$; C, 49.66; H, 4.40; N, 16.10 %. Found: C, 49.64; H, 4.39; N, 16.10 %.

Syntheses of complex [Zn(L)$(N_3)_2$] (2).

Complex **2** was synthesized following the same procedure as in the case of **1** replacing sodium thiocyanate with sodium azide (0.195 g, 3 mmol). Colourless single crystals suitable for X-ray analysis were obtained from the filtrate after a few days on keeping it in a $CaCl_2$ desiccator. (Yield: 69 %). Anal. Calcd.: $C_{16}H_{19}ZnN_9 \cdot 1/2H_2O$; C, 46.66; H, 4.61; N, 30.62 %. Found: C, 46.36; H, 4.39; N, 30.10 %.

Syntheses of complex [Cu(L)$(NCS)_2$] (3).

Complex **3** was synthesized adopting the same procedure as in the case of **1** replacing zinc perchlorate hexahydrate with copper perchlorate hexahydrate (0.370 g, 1 mmol). Colourless single crystals suitable for X-ray analysis were obtained from the filtrate after a few days on keeping it in a $CaCl_2$ desiccator. (Yield: 89 %). Anal. Calcd.: $C_{18}H_{19}CuN_5S_2$; C, 51.12; H, 4.49; N, 16.56 %. Found: C, 50.64; H, 4.09; N, 16.20 %.

Synthesis of complex [Ni (L)(2bpy)(NCS)](ClO_4)] (4).

Complex **4** was synthesized by following the same procedure as in the case of **1** using nickel perchlorate hexahydrate (0.365 g, 1 mmol) instead of zinc perchlorate hexahydrate. Light green single crystals suitable for X-ray analysis were obtained from the filtrate after a week. (Yield: 87 %). Anal. Calcd.: $C_{29}H_{28}N_5NiOS$, ClO_4; C, 53.35; H, 4.29; N, 10.73 %. Found: C, 53.20; H, 4.19; N, 10.53 %.

Caution: Perchlorate salts are explosive in nature, it should be handled with proper care.

X-Ray data collection and structure determination. The crystal structure of compound **3** was reported earlier (CCDC 758703).[39] The crystal structures of compounds **1**, **2**, and **4** were determined by X-ray diffraction methods. Intensity data and cell parameters were recorded at 296(2) K on a Bruker Smart AXS 1000 (MoKα radiation λ = 0.71073 Å) equipped with a CCD area detector and a graphite monochromator. Crystal data and experimental details for data collection and

structure refinement are reported in Table 3. Selected bond lengths and angles for **1**, **2**, and **4** are listed in Tables 1, 2, and 3, respectively. The high final R value for compound **1** is probably due to the low diffraction power of the crystal measured.

The raw frame data were processed using the SAINT and SADABS programs.[45] The structures were solved by direct methods using the SIR97 program[46] and refined on F_0^2 by full-matrix least-squares procedures, using the SHELXL-97 program.[47] All the non-hydrogen atoms were refined with anisotropic atomic displacements with the exception of a disordered carbon atom in compound **2**. The hydrogen atoms were included in the refinement at idealized geometries (C–H 0.95 Å) and refined "riding" on the corresponding parent atoms. The weighting schemes used in the last cycle of refinement were $w = 1/ [\sigma^2F_o^2 + (0.1554P)^2 + 9.4526P]$, $w = 1/ [\sigma^2F_o^2 + (0.0499P)^2 + 0.5208P]$, and $w = 1/ [\sigma^2F_o^2 + (0.0651P)^2 + 0.6597P]$, where $P = (F_o^2 + 2F_c^2)/3$, for **1**, **2**, and **4** respectively.

Crystallographic data (excluding structure factors) for the structure reported have been deposited with the Cambridge Crystallographic Data Centre as supplementary publication no. CCDC-1043274 (**1**), -1043275 (**2**), and -1043276 (**4**) and can be obtained free of charge on application to the CCDC, 12 Union Road, Cambridge, CB2 IEZ, UK (fax: +44-1223-336-033; e-mail deposit@ccdc.cam.ac.uk or http://www.ccdc.cam.ac.uk).

Table 1. Crystal data and structure refinement information for compounds **1**, **2** and **4**.

Compound	**1**	**2**	**4**
Formula	$C_{18}H_{19}ZnN_5S_2$	$C_{16}H_{19}ZnN_9 \cdot 1/2H_2O$	$C_{29}H_{28}NiN_5O_5SCl$
FW	434.87	411.78	652.78
Crystal system	Monoclinic	Triclinic	Triclinic
Space group	*P21/c*	*P-1*	*P-1*
a (Å)	8.886(2)	9.1391(5)	10.5195(6)
b (Å)	18.133(4)	9.3535(6)	12.7921(7)
c (Å)	13.793(3)	22.7690(10	13.6828(8)
α (º)	-	97.837(2)	62.887(2)

β (º)	106.672(4)	91.624(2)	68.064(2)
γ (º)	-	96.775(2)	87.976(3)
V (Å^3)	2129.0(8)	1912.8(2)	1499.8(2)
Z	4	4	2
T (K)	296(2)	296(2)	296(2)
ρ (g cm^{-3})	1.357	1.430	1.445
μ (mm^{-1})	1.360	1.307	0.852
F(000)	896	852	676
Total reflections	6925	25127	21968
Unique reflections (R_{int})	2703 (0.0283)	8961 (0.0219)	8844 (0.0317)
Observed reflections [F_o>4σ(F_o)]	2072	7036	5885
GOF on F^{2a}	1.050	1.067	1.008
R indices [F_o>4σ(F_o)]^b R_1, wR_2	0.0871, 0.2390	0.0349, 0.0930	0.0466, 0.1188
Largest diff. peak and hole (eÅ^{-3})	3.349, -0.427	0.424, -0.284	0.644, -0.489

[a]Goodness-of-fit S = [Σw(F_o^2-F_c^2)^2/ (n-p)]1/2, where n is the number of reflections and p the number of parameters. [b]$R_1 = \Sigma \| F_o | - | F_c \| / \Sigma | F_o |$, wR_2 = [Σ[w(F_o^2-F_c^2)^2]/Σ[w(F_o^2)^2]]$^{1/2}$.

Hirshfeld Surface Analysis. The non-covalent interactions present in the crystal structures of compounds **1-4** have also been studied by means of Hirshfeld surface analysis[48-50] carried out with the program Crystal Explorer.[51] All the distances involving hydrogen atoms have been normalized to standard neutron bond lengths.

Theoretical Methods. The energies of all complexes included in this study were computed at the BP86-D3/def2-TZVPD level of theory using the crystallographic geometries within the program TURBOMOLE version 6.4.[52] For the

calculations, we used the BP86 functional with the latest available correction for dispersion (D3).

Conclusions

In this present work, we have synthesized and structurally characterized four complexes that exhibit interesting features in the solid state. The formation of unconventional C–H···π interactions, where the π-system is provided by the pseudohalide coligand, are analyzed using DFT calculations, MEP surface and Hirsfeld analyses. In the case of NCS the interaction stems from the region of the central carbon atoms that exhibits a negative electrostatic potential On the contrary, in the case of the azide coligand the interaction involves the terminal nitrogen atom because the central nitrogen atom exhibits a positive potential. A rare ambidented behavior of the thiocyanato ligand in complex **3** has been explored ~~in the Cu-Schiff-base complex~~ and the origin of its genesis has been rationalized by DFT calculations. The photophysical behavior of all the complexes was also studied revealing the quenching and the enhancing effect of the paramagnetic and diamagnetic metal ion respectively, in presence of thiocyanate and azide as coligands.

Acknowledgement

The authors wish to thank CSIR, New Delhi [01(2464)/11/EMRII dt 16-05-11 to D.D.] for financial support and the University of Calcutta for providing the facility of a single crystal X-Ray diffractometer from the DST-FIST program. This work was supported by the DGICYT of Spain (project CONSOLIDER INGENIO 2010 CSD2010-00065, FEDER funds).

References

(1) C. A. Hunter, J. K. M. Sanders, *J. Am. Chem. Soc.*, 1990, **112**, 5525.

(2) C. Caltagirone, P. A. Gale, *Chem. Soc. Rev.*, 2009**, 38**, 520.

(3) A. Frontera, P. Gamez, M. Mascal, T. J. Mooibroek, J. Reedijk, *Angew. Chem., Int. Ed.* 2011, **50**, 9564.

(4) A. Frontera, *Coord. Chem. Rev*., 2013, **257**, 1716.

(5) J. A. Vargas, D. Emery, J. Mareda, S. K. Nayak, P. Metrangolo, G. Resnati, N. Sakai, S. Matile, *Nat. Commun.*, 2012, **3**, 905.

(6) M. M. Watt, M. S. Collins, D. W. Johnson, *Acc. Chem. Res.*, 2013, **46**, 955.

(7) P. A. Gale, *Chem. Commun.*, 2011, **47**, 82.

(8) M. Wenzel, J. R. Hiscock, P. A. Gale, *Chem. Soc. Rev.*, 2012, **41**, 480.

(9) P. A. Gale, R. Quesada, *Coord. Chem.Rev*., 2006, **250**, 3219.

(10) H. J. Schneider, *Angew. Chem. Int. Ed.*, 2009, **48** , 3924.

(11) H. J. Schneider, A. Yatsimirski, Principles and Methods in Supramolecular Chemistry, Wiley, Chichester, 2000.

(12) G. R. Desiraju, *Chem. Commun.*, 1997, **1475**.

(13) G. R. Desiraju, *J. Chem. Sci.*, 2010, **122**, 667.

(14) A. Tasada, F. M. Albertí, A. Bauza, M. B. Oliver, A. García-Raso, J. J. Fiol, E. Molins, A. Caubet, A. Frontera, *Chem. Commun.*, 2013, **49**, 4944.

(15) M. Mitra, P. Manna, S. K. Seth, A. Das, J. Meredith, M. Helliwell, A. Bauza, S. Ray Choudhury, A. Frontera, S. Mukhopadhyay, *CrystEngComm.*, 2013, **15**, 686.

(16) C.-S. Liu, P.-Q. Chen, E.-C. Yang, J.-L. Tian, X.-H. Bu, Z.-M. Li, H.-W. Sun and Z. Lin, *Inorg. Chem*., 2006, **45**, 5812–5821

(17) X.-He Bu, M.-L. Tong, H.-C. Chang, S. Kitagawa and S. R. Batten, *Angew. Chem. Int. Ed*., 2003, **43**, 192–195.

(18) (a) A. K. Rappé, E. R. J. Bernstein, *Phys. Chem. A*., 2000, **104**, 6117; (b) A. Hesselmann, G. Jansen, M. J. Schütz, *J. Am. Chem. Soc.*, 2006, **128**, 11730.

(19) (a) C. Adhikary, S. Koner, *Coord. Chem. Rev.*, 2010, **254**, 2933; (b) J. M. Epstein, B. N. Figgis, A. H. White, A. C. Willis, *J. Chem.Soc., Dalton Trans.*, 1974, 1954.

(20) S. Naiya, C. Biswas, M. G. B. Drew, C. J. Gómez-García, J.M. Clemente-Juan, A. Ghosh, *Inorg. Chem.*, 2010, **49**, 6616.

(21) P. Chaudhuri, T. Weyhermtiller, E. Bill, K. Wieghardt, *Inorg.Chim. Acta*., 1996, **252**, 195.

(22) J. Ribas, A. Escuer, M. Monfort, R. Vicente, R. Cortĕs, L. Lezama, T. Rojo, *Coord. Chem. Rev.*, 1999, **193**, 1027.

(23) S. Dalai, P. S. Mukherjee, T. Mallah, M. G. B. Drew, N. Ray Chaudhuri, *Inorg. Chem. Commun.*, 2002, **5**, 472.

(24) S. Mukherjee, B. Gole, Y. Song, P. S. Mukherjee, *Inorg. Chem.*, 2011, **50**, 3621.

(25) P. S. Mukherjee, T. K. Maji, A. Escuer, R. Vicente, J. Ribas, G. Rosair, F. A. Mautner, N. Ray Chaudhuri, *Eur. J. Inorg. Chem.*, 2002**,** 943.

(26) S. Mukherjee, Y. P. Patil, P. S. Mukherjee, *Dalton Trans.*, 2012**, 41**, 54.

(27) M. A. S. Goher, T. C. W. Mak, *Inorg. Chim. Acta*., 1985, **99**, 223.

(28) A. Escuer, G. Aromí, *Eur. J. Inorg. Chem.*, 2006, 4721.

(29) G. S. Papaefstathiou, S. P. Perlepes, A. Escuer, R. Vicente, M. Font-Bardia, X. Solans, *Angew. Chem., Int. Ed.*, 2001, **40**, 884.

(30) G. S. Papaefstathiou, A. Escuer, R. Vicente, M. Font-Bardia, X. Solans, S. P. Perlepes, *Chem. Commun.*, 2001, 2414.

(31) (a) S. R. Batten, K. S. Murray, *Coord. Chem. Rev.*, 2003, **246**, 103.
(b) D. Ghoshal, A. K. Ghosh, J. Ribas, E. Zangrando, G. Mostafa, T. K. Maji, N. Ray Chaudhuri, *Cryst. Growth Des.*, 2005, **5**, 941.

(32) (a) C. Sudbrake, H. Vahrenkamp, *Inorg. Chim. Acta*., 2001, **318**, 23.
(b) F. Gross, H. Vahrenkamp, *Inorg. Chem.*, 2005, **44**, 3321.
(c) R. Beck, U. Florke, H. F. Klein, *Inorg. Chim. Acta*., 2009, **362**, 1984.

(33) J. Miao, Y. Nie, C. Hub, Z. Zhang, G. Li, M. Xu, G Sun, *J. Mol. Struct.*, 2012, **97**,1014.

(34) C.A. Bessel, R. F. See, D. L. Jameson M. R. Churchill, K. J. Takeuchi, *J. Chem. Soc., Dalton Trans.*, 1992, 3223.

(35) K. F. Bowes, I. P. Clark, J. M. Cole, M. Gourlay, A. M. E. Griffin, M. F. Mahon, L. Ooi, A. W. Parker, P. R. Raithby, H. A. Sparkes, M. Towrie, *CrystEngComm*., 2005, **7** , 269.

(36) J. E. Beves, P. Chwalisz, E. C. Constable, C. E. Housecroft, M. Neuburger, S. Schaffner, J. A. Zampese, *Inorg. Chem. Commun.*, 2008**, 11**, 1009.

(37) S. K. Dey, G. Das, *Cryst. Growth Des.*,2010, **10**, 754.

(38) A. W. Addison, T. N. Rao, J. Reedijk, J. Vanrijn, G. C. Verschoor, *J. Chem. Soc.-Dalton Trans*., 1984, 1349.

(39) X. Q. Zhang, C.-Y. Li, H.-D. Bian, Q. Yu, H. Liang, *Acta Crystallogr.,Sect.E:Struct.Rep.Online,* 2009, **65**, 1610.

(40) P. Chakraborty, A. Guha, S. Das, E. Zangrando, D. Das, *Polyhedron*., 2013, **49**,12.

(41) R. A. Bailey, S. L. Kozak, T. W. Michelsen, W. N. Mills, *Coord. Chem. Rev.,* 1971**, 6**, 407.

(42) J. L. Burmeister, *Coord. Chem. Rev.,* 1990, **105**, 77.

(43) L. Vandenburgh, M. R. Buck, D. A. Freedman, *Inorg. Chem.*, 2008, **47,** 9134.

(44) F. H. Allen, *Acta Cryst., B***.,** 2002, **58**, 380.

(45) SAINT, Software Users Guide, v. 6.0, Bruker Analytical X-ray Systems, Madison, WI, **1999**; Sheldrick, G. M. SADABS: Area-Detector Absorption Correction, v. 2.03, University of Gottingen, Gottingen, Germany, **1999**; SADABS, v. 2008-1 **2008**.

(46) A. Altomare, M. C. Burla, M. Camalli, G. L. Cascarano, C. Giacovazzo, A. Guagliardi, A. G. G. Moliterni, G. Polidori, R. Spagna, *J. Appl. Crystallogr.*, 1999, **32**, 115.

(47) G. M. Sheldrick, SHELXL-97, Program for Crystal Structure Refinement, University of Gottingen, Gottingen, Germany, 1997; G. M. Sheldrick, *Acta Crystallogr. Sect. A* **.,**2008, **64**, 112-122.

(48) J. J. McKinnon, M. A. Spackman, A. S. Mitchell, *Acta Crystallogr.*, 2004, **60**, 627.

(49) J. J. McKinnon, D. Jayatilaka, M. A. Spackman, *Chem Commun.*, 2007, 3814.

(50) M. A. Spackman, D. Jayatilaka, *CrystEngComm.*, 2009, **11**, 19.

(51) S. K. Wolff, D. J. Grimwood, J. J. McKinnon, M. J. Turner, D. Jayatilaka, M. Spackman, Crystal Explorer, University of Western Australia, Crawley, version 3.1, Revision: 2012, 1448.

(52) R. Ahlrichs, M. Bär, M. Hacer, H. Horn, C. Kömel, *Chem. Phys. Lett.*, 1989, **162**, 165.

(53) S. B. Boys, F. Bernardi, *Mol. Phys.*, 1970, **19**, 553.